(2)

PL-TR-91-2099

CORRELATION OF SOLAR PARTICLE EVENTS WITH GEOMAGNETIC STORMS

U. DasGupta

Radex, Inc.
Three Preston Court
Bedford, MA 01730

January 31, 1991

Scientific Report No. 1

PHILLIPS LABORATORY
AIR FORCE SYSTEMS COMMAND
HANSCOM AIR FORCE BASE, MASSACHUSETTS 01731-5000

"This technical report has been reviewed and is approved for publication".

EDWARD C. ROBINSON
Contract Manager
Data Systems Branch
Aerospace Engineering Division

ROBERT E. McINERNEY, Chief
Data Systems Branch
Aerospace Engineering Division

FOR THE COMMANDER

C. NEALON STARK, Director
Aerospace Engineering Division

This report has been reviewed by the ESD Public Affairs Office (PA) and is releasable to the National Technical Information Service (NTIS).

Qualified requestors may obtain additional copies from the Defense Technical Information Center. All others should apply to the National Technical Information Service.

If your address has changed, or if you wish to be removed from the mailing list, or if the addressee is no longer employed by your organization, please notify GL/IMA, Hanscom AFB, MA 01731. This will assist us in maintaining a current mailing list.

Do not return copies of this report unless contractual obligations or notices on a specific document requires that it be returned.

Unclassified
SECURITY CLASSIFICATION OF THIS PAGE

REPORT DOCUMENTATION PAGE

1a. REPORT SECURITY CLASSIFICATION Unclassified	1b. RESTRICTIVE MARKINGS
2a. SECURITY CLASSIFICATION AUTHORITY	3. DISTRIBUTION/AVAILABILITY OF REPORT Approved for Public Release Distribution Unlimited
2b. DECLASSIFICATION/DOWNGRADING SCHEDULE	
4. PERFORMING ORGANIZATION REPORT NUMBER(S) RXR-91012	5. MONITORING ORGANIZATION REPORT NUMBER(S) PL-TR-91-2099
6a. NAME OF PERFORMING ORGANIZATION RADEX, Inc. — 6b. OFFICE SYMBOL (If applicable)	7a. NAME OF MONITORING ORGANIZATION Phillips Laboratory
6c. ADDRESS (City, State, and ZIP Code) Three Preston Court Bedford, MA 01730	7b. ADDRESS (City, State, and ZIP Code) Hanscom AFB Massachusetts 01731-5000
8a. NAME OF FUNDING/SPONSORING ORGANIZATION — 8b. OFFICE SYMBOL (If applicable)	9. PROCUREMENT INSTRUMENT IDENTIFICATION NUMBER Contract F19628-90-C-0090
8c. ADDRESS (City, State, and ZIP Code)	10. SOURCE OF FUNDING NUMBERS PROGRAM ELEMENT NO. 62101F; PROJECT NO. 7601; TASK NO. 22; WORK UNIT ACCESSION NO. RA

11. TITLE (Include Security Classification)

Correlation of Solar Particle Events with Geomagnetic Storms

12. PERSONAL AUTHOR(S)

U. DasGupta

13a. TYPE OF REPORT	13b. TIME COVERED	14. DATE OF REPORT (Year, Month, Day)	15. PAGE COUNT
Scientific Report #1	FROM 12/89 TO 12/90	1991, January 31	30

16. SUPPLEMENTARY NOTATION

17. COSATI CODES			18. SUBJECT TERMS (Continue on reverse if necessary and identify by block number)
FIELD	GROUP	SUB-GROUP	Solar particle events, energetic particles, solar flare, heavy ions, magnetic sudden commencements, geomagnetic storms, proton events, particle fluxes

19. ABSTRACT (Continue on reverse if necessary and identify by block number)

Solar particle events recorded by the DMSP/F7 Space Radiation Dosimeter and the IMP-8 Charged Particle Telescope have been studied. Some of the events were followed by geomagnetic storms while others were not. A detailed study of the particle components of these events was conducted in order to isolate differences in them that might be indicators of geomagnetic activity that follows some of the events. The advantage of finding such predictors is that the particle event precedes the magnetic activity by 1-2 days and would lead to an early warning for the impending storm. We found that events that were followed by magnetic storms had the following features that were different from events that were not followed by storms (1) A softer spectrum in the protons (2) A slower rise of the proton component from background to peak (3) More high energy electrons (above 1 MeV) than high energy protons (above 20 MeV). The first feature was verified in a sample of 11 solar particle events while (2) and (3) were confirmed using a sample of 5 events.

20. DISTRIBUTION/AVAILABILITY OF ABSTRACT ☒ UNCLASSIFIED/UNLIMITED ☐ SAME AS RPT. ☐ DTIC USERS	21. ABSTRACT SECURITY CLASSIFICATION Unclassified
22a. NAME OF RESPONSIBLE INDIVIDUAL E. C. Robinson	22b. TELEPHONE (Include Area Code) (617)377-3840 — 22c. OFFICE SYMBOL PL/LCY

DD FORM 1473, 84 MAR — 83 APR edition may be used until exhausted. All other editions are obsolete.

SECURITY CLASSIFICATION OF THIS PAGE
Unclassified

ACKNOWLEDGEMENTS

Dr. M. S. Gussenhoven of PHP initiated this investigation, and the progress of this effort benefitted greatly through her continuing interest, discussions, and support.

Thanks are due to Dr. J. King of NSSDC for providing IMP-8 solar proton data, and to Dr. W. Dietrich of the University of Chicago for the IMP-8 heavy ion data.

A note of appreciation also goes to Mr. D. Madden of Boston College for making the DMSP/F7 data as well as the access programs available.

TABLE OF CONTENTS

LIST OF FIGURES

LIST OF TABLES

1. INTRODUCTION

Solar particle events are caused by the acceleration and emission of energetic particles, mostly following the occurrence of a solar flare in an active region of the sun. A solar flare is accompanied by explosive heating and disturbance of the Sun's magnetic field. This produces a shock wave that accelerates particles to relativistic energies. At the Earth, the particle component observed consists primarily of electrons and protons, along with some heavy ions in about the same proportion as is present in the solar atmosphere. The relativistic particles reach the Earth within an hour following the occurrence of the solar flare. The associated shock, travelling at velocities of about 1000 km/sec, reaches the Earth 2 days later and is thought to cause magnetic sudden commencements.

The question of whether a solar event will be observed on the Earth depends on the location of the corresponding activity on the Sun. The solar particles emitted will follow the lines of the Archimedean spiral formed by the interplanetary magnetic field between the Sun and the Earth. The relativistic particles travel along the field lines with negligible lateral diffusion. Another factor determining whether a solar particle event will be detected is the energy threshold of the measuring instrument, since the particle components vary widely in flux and spectra. Typically, solar proton events have peak fluxes between 10 - 10^4 particles/(cm^2.sr.sec) above energies of 1 MeV [*Armstrong, et. al.*, 1989] while the spectral index varies between 1.0 and 3.2 at energies above 1 MeV. The average solar particle event lasts a few days, exhibiting a sharp rise in the flux followed by a gradual fall off. The spectrum is hardest at the beginning of the event and becomes softer towards the end. We find that the change in the spectral hardness of the particles in a solar event is a much better indicator for the occurrence of the event than is the change in the overall flux of the particles.

Solar flares are responsible for a number of geophysical disturbances, among them magnetic storms. A geomagnetic storm can be described as a sudden, abrupt change in the geomagnetic field. The field variations occurring during a storm are complicated and highly variable. However, it is possible to generalize a magnetic storm as consisting of three distinct phases. The first is the sudden commencement phase where there is a sharp change in the magnetic field of tens of nanoteslas. This is followed by the main storm phase where the magnetic field decreases by 100 nT or more over a period of a few hours up to a day. Finally, during the relaxation phase the field changes quickly over a few days followed by a long recovery period where it could take the field a few months to relax to the prestorm level. It is generally believed that a sudden storm commencement is caused due to the impulsive compression of the magnetosphere by the passage of a shock front. We have noticed that for solar particle events where a sudden impulse was recorded, the impulse occurred within a few hours following particle onset and about a day **before** the arrival of the shock front. This indicates that magnetic sudden commencements are related to the particle component of the flare rather than its associated shock. This will be discussed later.

Finally, there is the question of magnetic storm prediction. There have been many attempts at forecasting the advent of magnetic storms on Earth. This effort is important since these storms carry many hazards - chiefly the disruption of communications and heating of the ionosphere. So far, no unique set of conditions has been discovered that would predict the occurence of a magnetic storm. It is generally believed that the arrival of particle shock at the magnetosphere together with a southward turning of the interplanetary magnetic field are necessary conditions for the precipitation of a magnetic

storm. But the problem with using the IMF or plasma shock as indications of storm commencement is that one cannot predict the storm until the conditions are right for its onset.

We have attempted a different approach to this problem. We studied solar proton events that were followed by geomagnetic storms and ones that were not followed by any apparent geomagnetic activity in an effort to examine differences in the particle components that might indicate if a magnetic storm would or would not follow. Since a magnetic storm lags its associated particle event by about 2 days, any indicators for the storm that are found in the particle component would lead to an earlier prediction of the storm than is currently possible. In our study of solar particle events, many of which were followed by magnetic activity, we observed dramatic differences between the class of events where the magnetosphere is quiet and those where it is disturbed. These differences in the particle components are noticed even when the magnitude of disturbances is modest - an overall increase of the ring currents translating to a decrease in the Dst indices of 50 nT or so over the prestorm level. We shall present the results of this study later.

One aspect of our study deals with the entry of particles into the magnetosphere from external sources. The flux profiles in a solar proton event were compared inside and outside the magnetosphere using the results of the dosimeter on the DMSP/F7 and the proton telescope aboard the IMP-8 satellite. The particle components of a solar event directly follow interplanetary field lines that connect to open geomagnetic field lines at higher latitudes. Due to the fact that flux profiles of a solar particle event observed over the polar caps of the Earth closely resemble those observed outside the magnetosphere, the process of diffusive entry is ruled out. A direct mechanism of entry of solar particles into the magnetosphere is indicated. The particle entry into the magnetosphere should then carry information regarding the state of connectedness between the inside and outside of the magnetosphere. Our purpose is to investigate any differences in the particle components that might result from changes in the connection when there is a storm.

2. INSTRUMENT DESCRIPTION AND DATA REDUCTION

Solar particle data were obtained from two instruments - the Space Radiation Dosimeter (SSJ*) on board the DMSP/F7 satellite and the Charge Particle Measurement Experiment (CPME) on the IMP-8 satellite.

2.1 DMSP/F7 SSJ*

The DMSP/F7 is a polar orbiting satellite at an altitude of 840 km. It has a 1.7 hr period and a noon-midnight meridian orbit plane. The Space Radiation Dosimeter on board the satellite consists of four particle detectors placed behind various thicknesses of aluminum shielding, which place the energy threshold of detection of protons at 20, 35, 51 and 75 MeV, and that for electrons at 1, 2.5, 5 and 10 MeV (Figure 1; Table 1). Details of the instrument construction and calibration can be found in Gussenhoven, et. al., [1986].

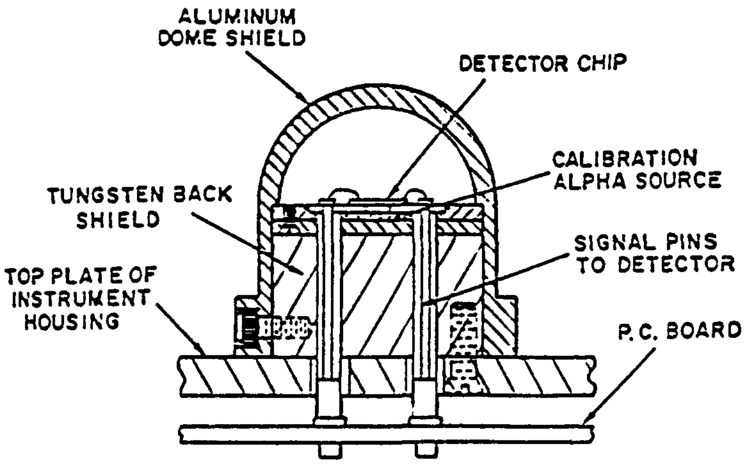

Figure 1. Schematic of one of the four sensors of the DMSP/F7 Space Radiation Dosimeter

TABLE 1. DMSP/F7 SSJ* Instrument Specification

	Aluminum	Range Thresholds		Detector	
Dome	Shield (gm/cm^2)	Electrons (MeV)	Protons (MeV)	Area (cm^2)	Thickness (microns)
1	0.55	1.	20	0.051	398
2	1.55	2.5	35	1.000	403
3	3.05	5.	51	1.000	390
4	5.91	10.	75	1.000	384

In each detector of the SSJ* instrument, particles are separated according to their total energy loss in the detector. The three ranges of energy deposit are the LOLET between 0.05 and 1 MeV, the HILET between 1 and 10 MeV and the VHLET where a total energy deposit of at least 40 MeV is required (75 MeV for detector 3). The flux of particles depositing the required amount of energy in each of the detectors is counted, as well as the cumulative dose resulting from the passage of the particles through the detector. The LOLET channels record electrons and high energy protons (energy greater than approximately 120 MeV) while the HILET channels mostly see protons. The VHLET channels are sensitive only to large deposits of energy from nuclear "star" events, from the passage of heavy nuclei through the detector, or from protons with a very long path length in the detector.

Dosimeter Data Specification: The dosimeter measures HILET, LOLET and VHLET particle count rates in 4 second time bins. Hourly averages of the data were determined after applying two sets of cuts. In order to eliminate the effect of the trapped particle populations, count rates were averaged over latitudes above 50° for protons, while in the case of electrons this was done at latitudes higher than 70°. A further condition was imposed in that each averaging interval contain at least 170, 4 second measurements of the particle fluxes. This ensures a coverage of at least half of a polar cap crossing over an hourly average. This step prevents the latitudinal variation of particle flux levels over the polar cap from obscuring the temporal variations in the particle profiles due to a solar event.

The Dosimeter was operational between December 1983 and February 1988. Solar particle events recorded during that time were isolated for a detailed study.

2.2 IMP-8 CPME

The Johns Hopkins University/Applied Physics Lab's Charged Particle Measurement Experiment (CPME) has been operating on board the IMP-8 satellite since 1973 (Figure 2). Details of the experimental construction and calibration can be found in Krimigis, et. al. [1973]. The IMP-8 satellite has an almost circular orbit whose distance of closest approach to Earth is 29 Earth radii and as such it spends a large part of its time outside the magnetosphere. The instrument records protons in 10 energy channels between 0.3 and 138 MeV, alpha particles in 6 energy channels between 0.64 and 52 MeV/nucleon and 3 channels of electrons spanning the range 0.22 to 2.5 MeV. The data for the CPME experiment were obtained from the NSSDC data bases. They represent omnidirectional hourly averaged integral fluxes of protons above 1, 2, 4, 10, 30 and 60 MeV.

Since the SSJ* and CPME experiments detect protons inside and outside the magnetosphere respectively, in similar energy ranges, comparisons between solar events seen by both instruments yield information regarding particle entry onto the polar caps from outside the magnetosphere.

The study of the data is divided into two parts. In the first part we study 11 major solar proton events that were recorded by the proton telescope on board the IMP-8 satellite between December 1983 and February 1988. Of these 11 events, one had a rather soft spectrum which rendered it undetectable above 20 MeV threshold of the DMSP/F7 dosimeter while five of the other events had bad or missing data giving an overall sample of 5 good events in the dosimeter. Both the proton and electron components of these five events are studied in detail in the second part of the data analysis.

3. RESULTS FROM IMP-8 CPME

A summary of the characteristics of the 11 proton events recorded by the CPME detector is presented in Table 2. The table also includes the geomagnetic activity expressed by the Dst index, during the particle events. The magnetic data were obtained from NSSDC online Interplanetary Medium (OMNI) data bases. The second and third columns of Table 2 list the time of occurrence of the peak in the solar proton event and the flux above 1 MeV at peak, as measured by the IMP-8 proton telescope. The fourth column gives the spectral index at the maximum of the flux. This index is derived by fitting the

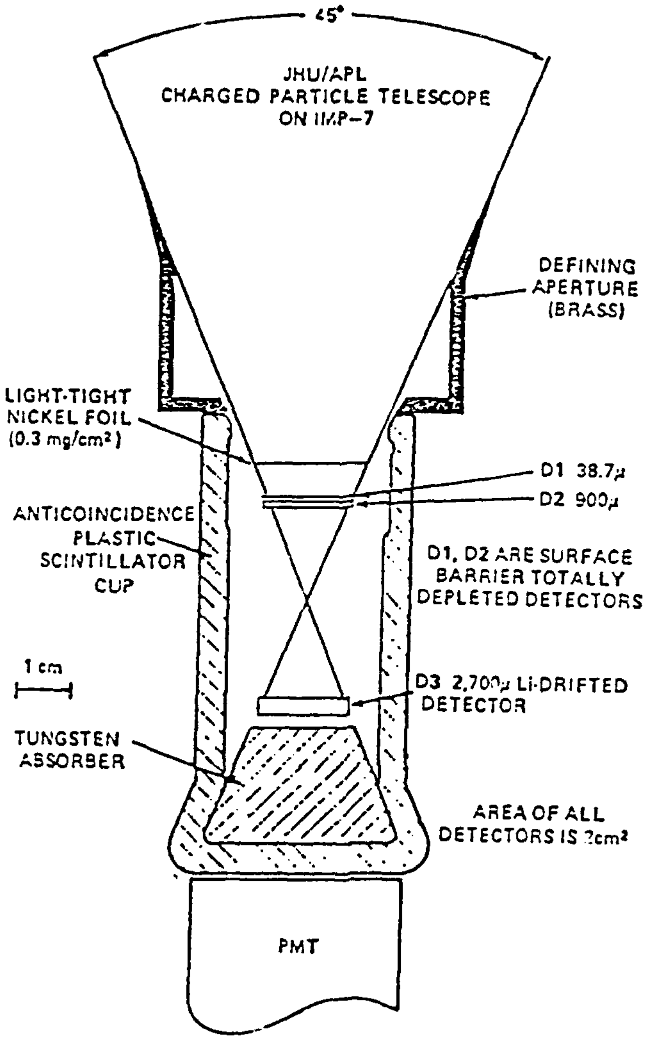

Figure 2. Construction of the IMP-8 Charged Particle Measurement Experiment

TABLE 2. Solar Proton Events from IMP-8 CPME

No	Time of start of particle event	Proton Component [CPME/IMP-8]			Magnetic Activity	
		Time of peak Date : Hour	Flux at peak (>1 MeV) /(cm^2.sr.sec)	Spectral index at peak	Time of minimum Dst Date : Hour	Min. Dst (nT)
1	Feb 16, 84	Feb 16 : 11.5	309.3	-1.08	--	--
2	Mar 12, 84	Mar 14 : 9.5	290.8	-1.93	--	--
3	Apr 25, 84	Apr 26 : 17.5	12320	-1.98	Apr 26 : 3.5	-93
4	Apr 24, 85	Apr 26 : 4.5	6812	-2.62	Apr 28 : 11.5	-99
5	Jul 09, 85	Jul 09 : 7.5	410.3	-2.25	Jul 12 : 19.5	-66
6	Feb 06, 86	Feb 08 : 15.5	5448	-3.19	Feb 09 : 0.5	-312
7	Feb 14, 86	Feb 15 : 3.5	1443	-1.89	--	--
8	Nov 02, 86	Nov 04 : 0.5	8225	-4.91	Nov 04 : 10.5	-109
9	May 29, 87	May 30 : 4.5	28.2	-2.44	May 31 : 22.05	-62
10	Nov 07, 87	Nov 08 : 10.5	1420	-2.17	--	--
11	Dec 29, 87	Dec 29 : 13.5	226.8	-1.48	--	--

differential flux to a power law type spectrum of the form $dN/dE = CE^{\gamma}$ where dN/dE is the number of protons per unit energy interval at the energy E. The values of γ in the last column represent the spectral hardness of the proton event between 1 and 10 MeV.

The last two columns in the table list geomagnetic activity during the events. If evidence of the onset of a magnetic disturbance is found between 1-3 days following the start of a particle event, the minimum recorded Dst over the episode, as well as the time of occurrence of the minimum, are listed in the last two columns of Table 2.

There is one trend that we notice outright from the data. Proton events that are followed by magnetic storms have a softer spectrum in general than the ones that have no magnetic activity associated with them. The spectral indices for the storm related proton events lie between -1.98 and -4.9, while the rest have a much flatter spectra ranging between -1.1 and -2.2.

4. RESULTS FROM DMSP/F7 SSJ*

Five out the eleven proton events detected by the CPME experiment have been recorded by the DMSP dosimeter. We shall start by analyzing two of the solar events in detail. These occurred on February 6th and February 14th, 1986. The hourly averaged value of the proton count rates above 20 MeV and the electron count rates above 1 MeV measured by the DMSP dosimeter are plotted in Figure 3a. The uniqueness of these two events lies in the fact that while both were fairly large events (peak proton fluxes 5.4×10^3 and 1.4×10^3 above 1 MeV, respectively) they occurred close to solar minimum. This indicates that although flare occurrences on the sun and the resultant incidence of particle events is less frequent at solar minimum, the magnitude of individual events has little to do with the level of solar activity. Anomalously large solar particle events have been observed at solar minimum, such as one occurring on August 4th, 1972 in the minimum of solar cycle 20 (see for example, King [1974]). Another remarkable feature of the February, 1986 events was that although they occurred close together in time, the first event was followed by an extraordinarily large geomagnetic storm for which the Dst index reached a minimum value of -312 nT, while the second event was not associated with any discernible magnetic activity. We shall therefore try to investigate any differences in the two particle events which might indicate why the first event was followed by a magnetic storm while the second event was not. The sample of the three remaining particle events is used for a verification of the storm predictors found from the comparison of the two February 1986 solar particle events.

5. EVENTS 6 & 7: FEBRUARY 6 AND FEBRUARY 14, 1986

We shall begin a detailed comparison of the February 6th and February 14th events by looking first at the latitudinal variations of the particle components during both events. This will be followed by a comparison of the DMSP/F7 particle flux measurements made over the polar caps with the interplanetary values obtained from the IMP-8 instruments. Finally, different aspects of the flares that led up to and occurred during the two particle events are compared, as well as the geomagnetic activity occurring during the two events.

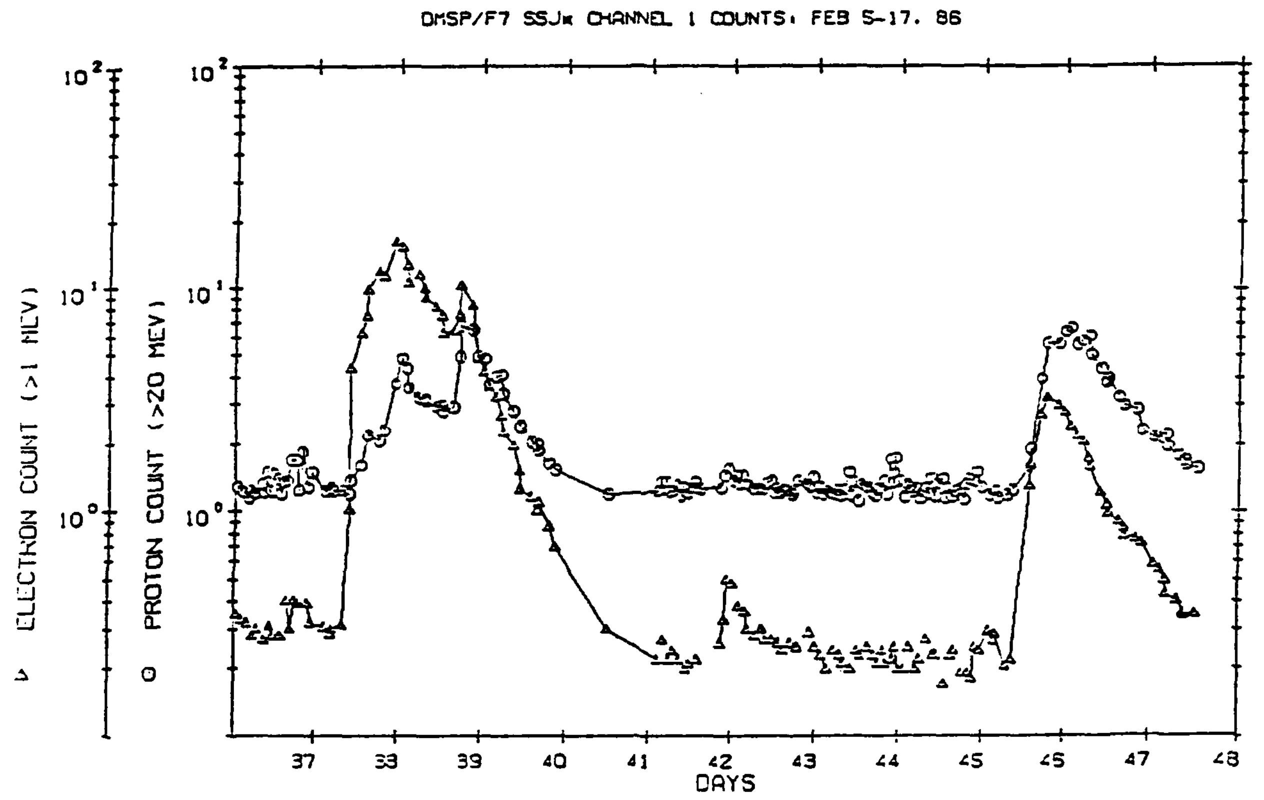

Figure 3a. Proton and electron count rates in DMSP/F7 SSJ* instrument during solar particle events

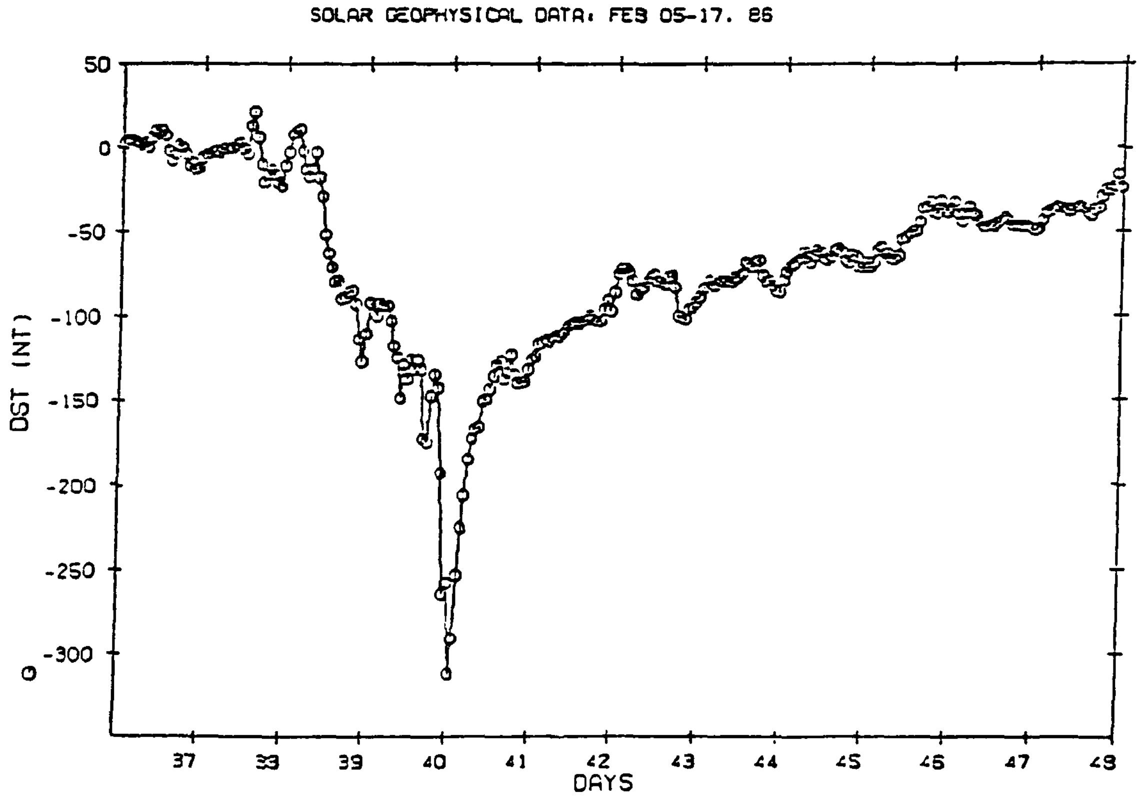

Figure 3b. Dst indices over the time period of February 6th and 14th, 1986.

5.1 LATITUDINAL DEPENDENCE OF PARTICLE FLUXES

Being in a 99° inclination orbit, the DMSP/F7 spends a fair fraction of its time over the Earth's polar caps. At these higher latitudes, particles from external sources can gain direct entry into the Earth's magnetosphere. Figure 4a gives the proton count rate above 20 MeV averaged over 5° bins in the latitude over the time of the first solar event between February 6th and 9th (circles) and the quiet time in between the two particle events, i.e. February 10th - 14th (triangles). Over the first time period, both the particle components and the accompanying magnetic storm had reached their peak values.

We notice that in quiet times, the particle flux profiles are fairly flat over both polar caps. During the solar event, protons start to gain access at around 50° north and south latitudes. There is a peak in the proton fluxes at 65° followed by a flattening off of the flux. In Figure 4b, the quiet time profile is compared to that over the second proton event between February 14th and 17th. We notice that the variation of the proton flux with latitude is the same as for the previous case, except, possibly, for a sharper fall off in the flux over the north pole.

Next we compare the flux profile of high energy electrons over the DMSP orbit for the first event (5a) and the second event (5b), in both cases using the quiet period in between the two events as the common baseline. In Figure 5a, we notice that the electron count rate is fairly unperturbed over the inner belts, but that the outer belts, extending between a latitude of 40° and 70°, are perturbed by electron entry during the solar event. Both the equatorial and polar boundaries of the outer electron belt were at higher latitudes. In both hemispheres, the polar edges of the belt shift by about 2°-3° degrees while the equatorial edge sees a more dramatic shift of 7° in the northern hemisphere and 10° in the southern hemisphere. The profile over the polar caps is flat in both cases. Figure 5b represents the flux profiles during the second particle event. Here, we notice the same poleward shift in the outer zone electrons, though the migration in this case is modest for both edges of the belt in both hemispheres, about 1°-4°.

To summarize, the latitudinal dependence of the proton component of a particle event seems to show little change with the level of geomagnetic activity. On the other hand, electron entry into the magnetosphere appears to be sensitive to the presence of the magnetic storm.

5.2 COMPARISON OF POLAR CAP AND INTERPLANETARY PROTON FLUX MEASUREMENTS

In Figure 6, the proton flux inside and outside the magnetosphere during the two solar events are compared at 30 MeV and 60 MeV. The closed circles give the values measured by the DMSP/F7 dosimeter averaged over the polar caps (>50° magnetic latitude) and interpolated to 30 MeV and 60 MeV. The flux measurements of IMP-8 (open circles) represent interplanetary values.

We notice some obvious differences between the two measurements. The DMSP/F7 measured flux values are consistently lower, indicating that protons do not gain total access to the polar cap region. The best agreement between the two measurements is at the onset and at the peak of the events, although we do notice that the low altitude measurements show a greater fluctuation at the beginning of the events, indicating that the protons are alternately being allowed and denied access to the polar caps. This effect

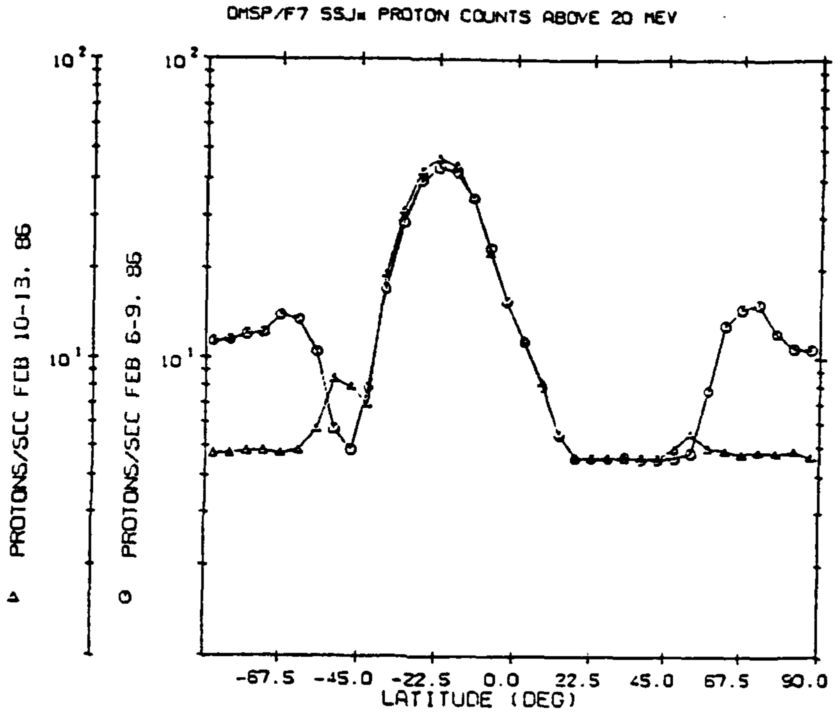

Figure 4a. Latitudinal variation of proton fluxes during a particle event between February 6-9 and a quiet time February 10-13.

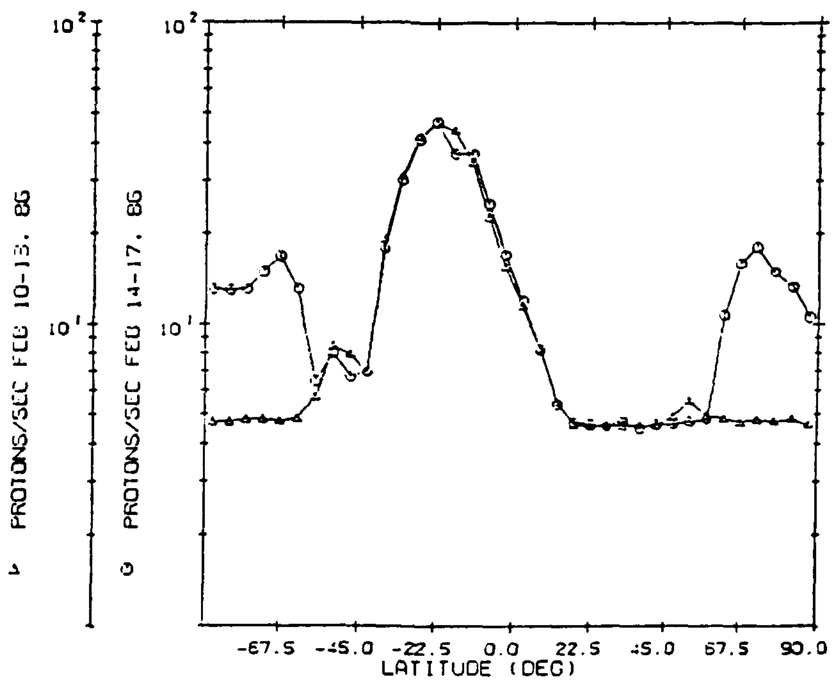

Figure 4b. Particle event between February 14-17 compared to the same quiet period.

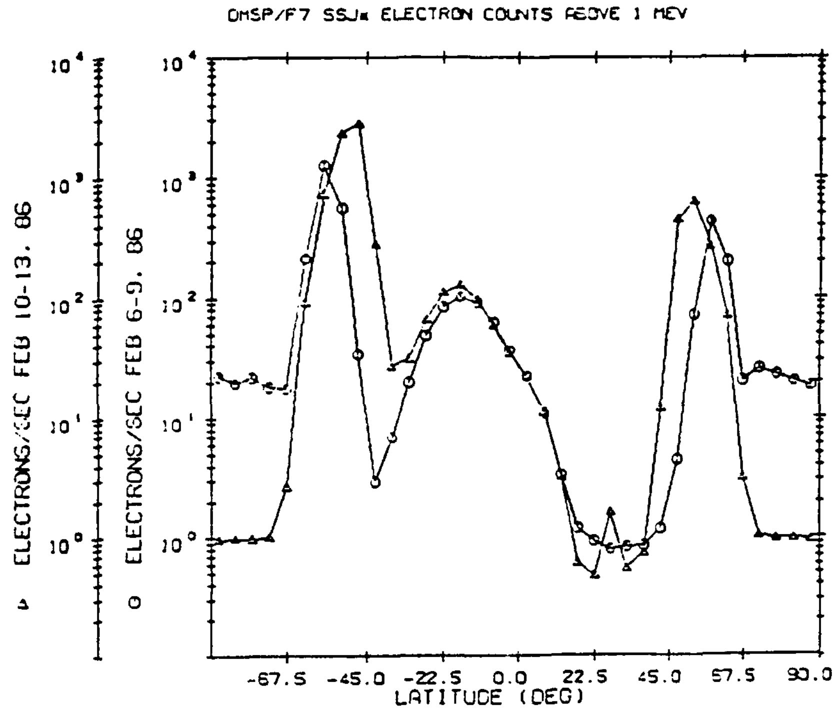

Figure 5a. Latitudinal variation of electron fluxes during a particle event between February 6-9 and a quiet time February 10-13.

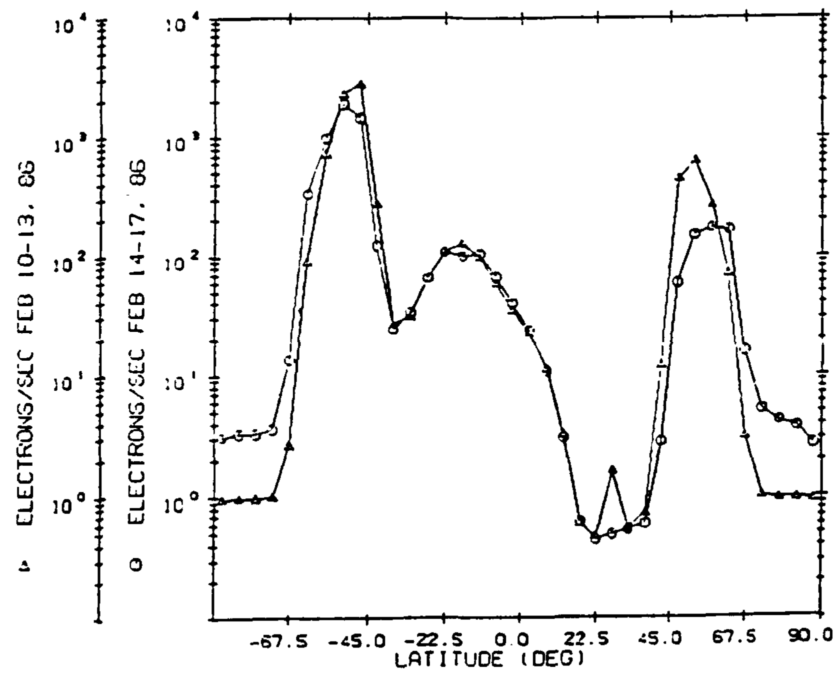

Figure 5b. Particle event between February 14-17 compared to the same quiet period.

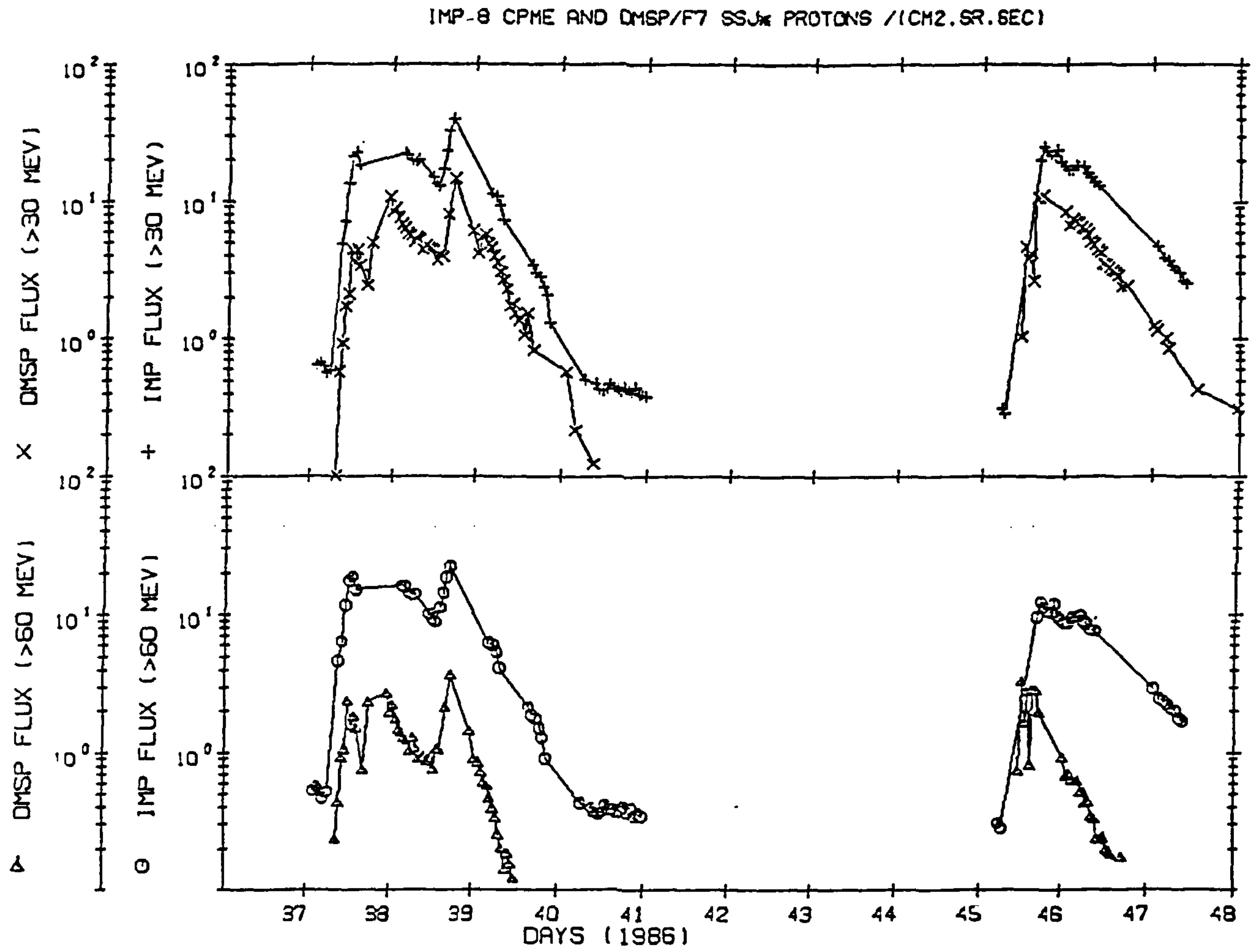

Figure 6. Comparison of protons fluxes measured over polar caps by DMSP/F7 Dosimeter with interplanetary values recorded by IMP-8 Proton Telescope at 30 MeV and 60 MeV.

has been observed by Van Allen, et. al. in their comparisons of proton data from the Injun 5 and the Explorer 33 satellites [*Van Allen, et. al.*, 1971]. We also notice that the divergence in the two sets of measurements increases towards the end of the event. Since the spectrum also gets softer towards the end of the event, this implies that less higher energy protons gain access to the polar caps than lower energy ones. Next, we compare the flux profiles at 30 MeV with those at 60 MeV. A smaller fraction of the protons at 60 MeV are able to get into the magnetosphere than those at 30 MeV. This further supports the fact that higher energy protons are denied access to the polar cap regions. A likely explanation for this fact is the presence of a filamentary structure in the geomagnetic field which produces a better collimation of the lower energy protons.

If we compare the two events, we find that in the first event 37% of the protons with energies above 30 MeV and 17% of those above 60 MeV gain access to the Earth over the poles. In the case of the second event, these numbers are 42% and 23%, respectively. We notice that fewer solar protons are detected at the Earth during the first event, indicating a disruption in particle entry due to the geomagnetic storm that reaches its peak during the first event.

5.3 COMPARISONS OF FLARE RELATED QUANTITIES

Next, we study the temporal variations in a number of flare related phenomena that occurred at or around of the time of observation of the particle events. The profiles of the different components are plotted in Figure 7 between February 5th and 18th, 1986. The phenomena are presented in the chronological order of their observation at the Earth. The top graph gives the electron count rate above 1 MeV obtained from the SSJ* experiment, while the second one gives the proton count rate above 20 MeV. Both are measured in the first detector of the dosimeter. The two proton events are similar in total intensity and duration. Both events show a quicker leading edge compared to the fall off, although the first event has a much slower rise time than the second, and it also exhibits a curious two peak structure. The arrows at the top of the graph indicate the occurrences of Xray flares of type M or stronger. All of the flares are clustered around one of the two particle events. In each case, we notice that there are 2-3 precursor flares with the onset of the particle event following the strongest of the Xray flares in the series.

Magnetic sudden commencements, indicated by arrows at the bottom of the second plot, followed the start of both particle events by 3-4 hours.

The third graph depicts the solar wind speed as a function of time. There is distinct evidence of a shock arrival following the first particle event. There are no data available over the time period of the second event.

In the last two graphs, the Kp and Dst indices reveal the geomagnetic activity during the time period of the two events. We notice a huge magnetic storm during the Feb 6th event, but no activity during the time of the second event.

The chart on the right side gives the time sequencing of the various events. The X-ray flare is followed in about an hour by the arrival of the electron component at the Earth. The protons trail the electrons by another hour or so. The magnetic sudden commencements occur a few hours following particle onset

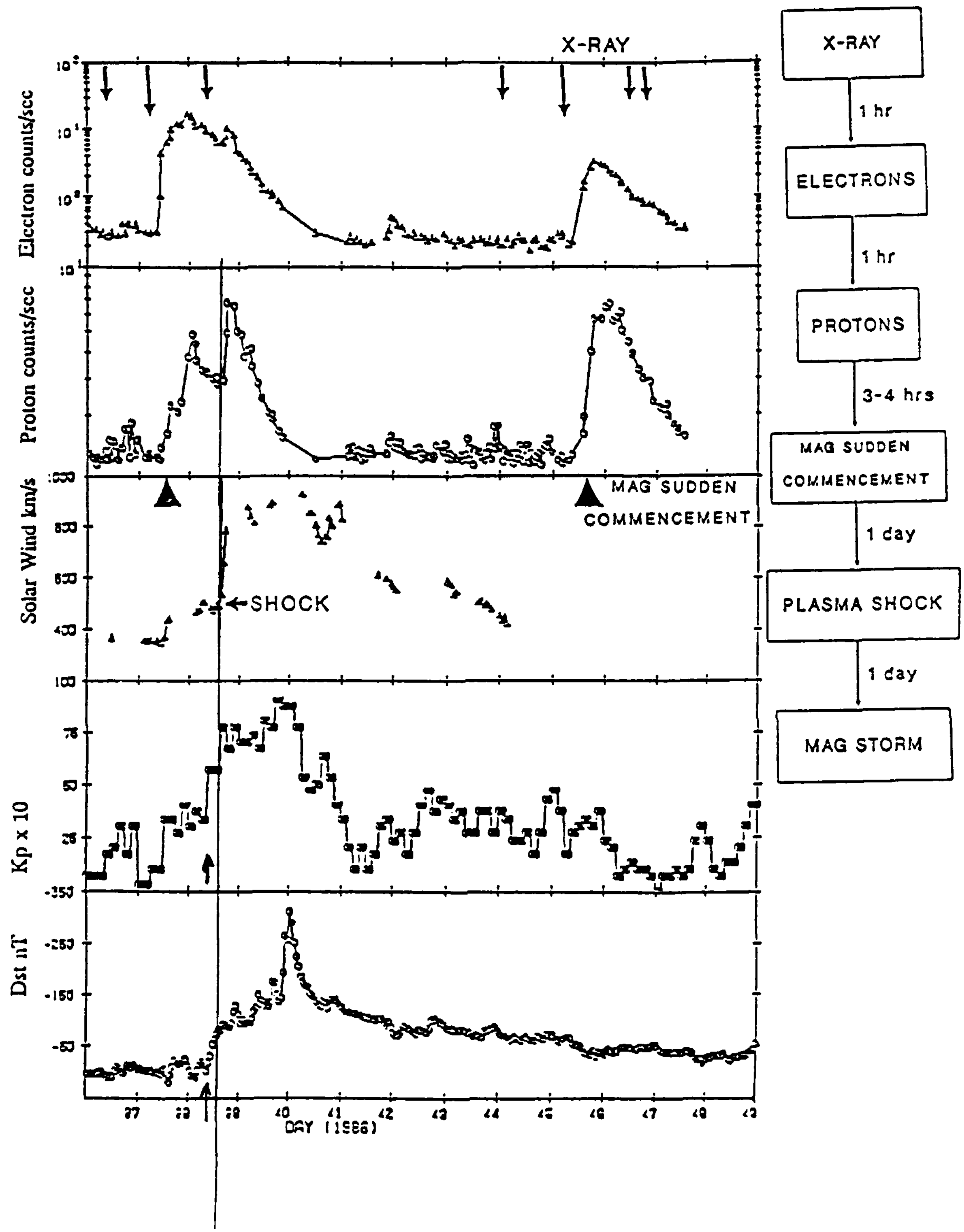

Figure 7. Plots of the proton and electron component, solar wind plasma, Kp and Dst indices between February 5th and 18th, 1986. The occurrence of Xray flares and sudden commencements are also indicated.

while the solar wind plasma shock arrives a day or so later. The magnetic storm develops shortly after the arrival of the shock plasma and reaches a peak a day later.

An important observation can be made from the preceding investigation. The magnetic storm develops 1-2 days following the arrival of the particle components at the Earth. If one were to find signatures in the particle events that might indicate that a magnetic storm would follow, one would have a lead time of a day or two in avoiding the hazards that might occur with the storm. It is generally believed that the arrival of a plasma shock, together with a southward IMF, will lead to a geomagnetic storm. These are not the best indicators for most practical purposes because the storm sometimes occurs concurrently with the southward turning of the IMF, so that no advance warning is obtained.

We now investigate major differences in two events to find features that might be significant enough to be used as pointers to the fact that the first event led to or caused a geomagnetic storm, while the second one did not. A comparison of the two particle events is summarized in Table 3. We notice that the first event was preceded by a stronger X-ray flare than the second, but this is not very significant since there have been larger recorded flares that have not led to magnetic storms, with the converse also being true in that there are major magnetic storms that are not flare related [*Smith and Smith*, 1963]. Both particle events are followed within an hour of their arrival at the Earth by magnetic sudden commencements (SCs) indicating that the appearance of SCs does not necessarily herald the onset of a magnetic storm. However, if we look at the particle components of the two solar events, some significant differences emerge. The first is that the spectrum of protons is softer in the first event. The second difference is the rise time of the proton component from the background to peak value, which is about twice as long for the first event as it is for the second. Also, the profile of the rising edge is considerably more bumpy in the first case, while it is fairly smooth in the second case. However, the profiles and rise time of the electron component is similar in both cases. Next, we compare the actual fluxes of protons and electrons above 20 MeV and 1 MeV, respectively. Since both sets of counts are recorded by the same detector, the geometrical factors are the same. We note that the first event contains considerably more electrons than protons with energies greater than the thresholds specified above, while the reverse is true for the second event. Finally, we notice that the fraction of protons gaining access to the polar caps is somewhat smaller during the first event.

In conclusion, we find that there are three important differences in the particle components of the event that was followed by a magnetic storm and the one that was not. The first is that the spectrum of particles at peak is softer in the event that preceded the magnetic storm. The second is that the time taken for the proton component to rise to maximum is considerably slower for this event. Also, there are proportionately more high energy electrons than protons. In the following section we shall investigate three other events (numbers 1, 2, 3 in Table 2). The first two were not followed by any geomagnetic activity, while the third one was.

5.3.1 Event 1: February 16th, 1984

The particle event of February 16th, 1984 (Figure 8) shows a quick rise to the peak (less than an hour) for both protons and electrons. The peak fluxes for both components are the same, although the electrons, in this case, die out much quicker than the protons - over a period of about 2.5 days. In the period following the event, the Dst index remains predominantly positive, indicating the absence of magnetic storm activity.

TABLE 3. Comparison of Solar Particle Events of February 6th and 14th, 1986

	Event 1: Feb 6-9, 1986	Event 2: Feb 14-16, 1986	Reference
Particle Events	1. Softer proton spectrum: Differential index of 1 MeV protons at peak = -3.19	= -1.89	IMP-8 CPME data
	2. Slower rise time of protons from start of event to peak. Rise time = 33 hrs 5 mins	= 14 hrs 15 mins	DMSP/F7 SSJ* data
	3. Larger electron flux compared to protons: Peak electron/Proton counts = 3.0	Smaller electron flux: = 0.4	DMSP/F7 SSJ* Electron >1 MeV Proton >20 MeV
	4. Total heavy ion fluence about the same: 54 CNO (21-43 MeV), no Fe (47-80 MeV)	32 CNO, 4 Fe	IMP-8 U. of Chicago Heavy Ion Experiment
	5. Same total dose in flare Total dose = 8.5 rads	= 8.9 rads	DMSP/F7 SSJ*, Detector 1 dose
	6. Fewer protons gain access to polar caps. 37% above 30 MeV 17% above 60 MeV	42% above 30 MeV 23% above 60 MeV	IMP-8 and DMSP/F7 solar proton data
X-ray Flares	7. Particle event followed X1.7 class X-ray flare	Event followed M6.4 flare	GOES 6 X-ray data
	8. 3 precursor flares between February 3-5 (1 during proton event)	3 precursors (2 during proton flare)	GOES 6 X-ray data
Solar Wind Plasma and Magnetic Activity	9. Substantial increase in solar wind speed (shock arrival)	No data	NSSDC OMNI data
	10. Magnetic sudden commencements following particle events February 6th, 13:12	February 14th, 14:34	Solar Geophysical Data Prompt Reports
	11. Accompanied by strong geomagnetic storm (largest in 30 yrs)	No storm observed	NSSDC OMNI data

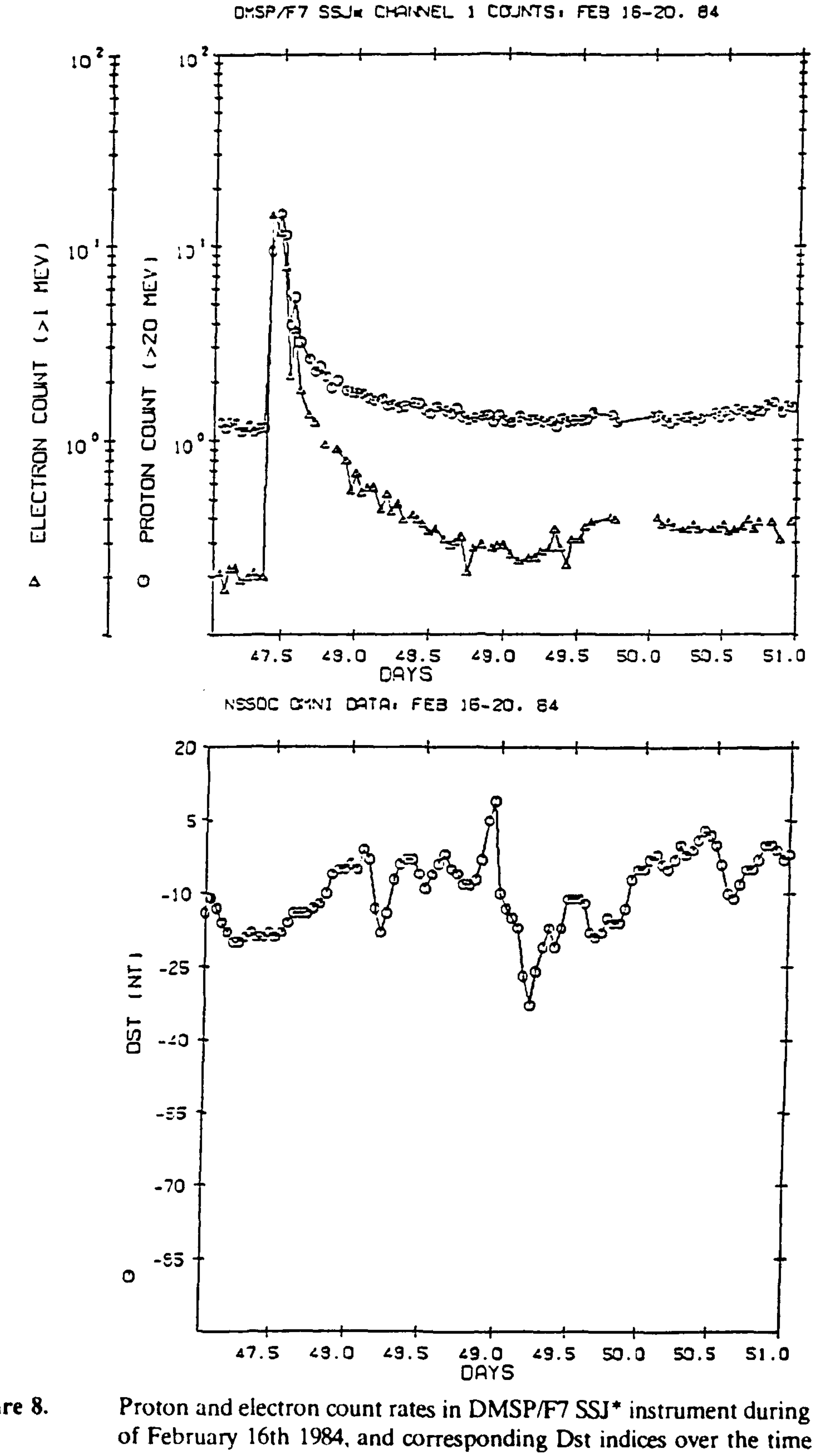

Figure 8. Proton and electron count rates in DMSP/F7 SSJ* instrument during solar particle event of February 16th 1984, and corresponding Dst indices over the time period.

5.3.2 Event 2: March 12th, 1984

This event (Figure 9) is similar to the previous one in its particle profiles. We notice the same sharp rise from the quiet time count rate to the peak. The flux of protons above 20 MeV is comparable to that of electrons above 1 MeV. Again, the magnetosphere is quiet following this event.

5.3.3 Event 3: April 26th, 1984

This solar particle event (Figure 10) is distinctly different from the two previous ones. The protons and electrons rise to their peak value over a period of about 2 days. In addition, there are about 5 times as many electrons above 1 MeV as there are protons above 20 MeV. Following the particle event is a geomagnetic storm that reaches a minimum Dst of almost -100 nT.

We observe that the differences seen in the particle events of February 6th and 14th, 1986 are borne out in the three events in 1984.

6. DISCUSSION AND CONCLUSIONS

In this study, we have not attempted to uncover underlying causes that lead to the precipitation of a geomagnetic storm following a solar particle event, but rather we have pursued an empirical approach to the problem where we studied solar particle events that were followed by geomagnetic storms and ones that were not. We identified consistent differences in the particle components of these two classes of events. Over the polar caps, we noticed that the ratio of high energy electrons to high energy protons was higher in the particle events that were followed by geomagnetic storms. These events also exhibited a longer rise time for the protons, though not for the electrons, suggesting that it is the proton entry onto the polar caps that is inhibited during events that are associated with magnetic activity. This observation is borne out in a comparison of the interplanetary fluxes of the protons during particle events with those measured at low altitudes over the poles. Less protons are seen to gain access to the polar caps when there is a magnetic storm. Also, the spectrum of the protons is considerably softer for the storm related events, indicating a preferential access of the lower energy protons in these events. We have verified the above features in a data sample of events spanning half a solar cycle with corresponding particle events of different sizes and energy thresholds.

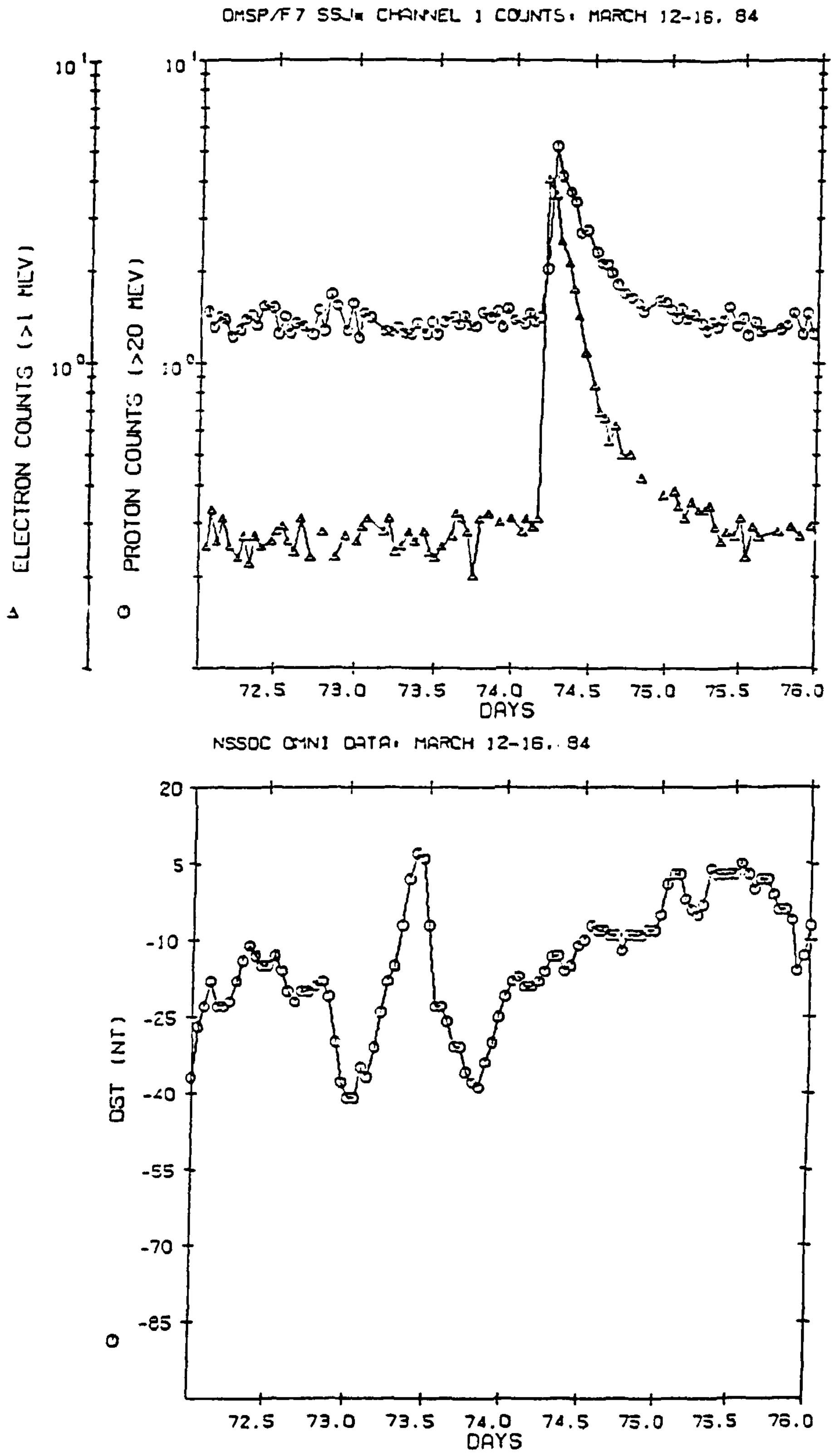

Figure 9. Proton and electron count rates in DMSP/F7 SSJ* instrument during solar particle event of March 14th 1984, and corresponding Dst indices over the time period.

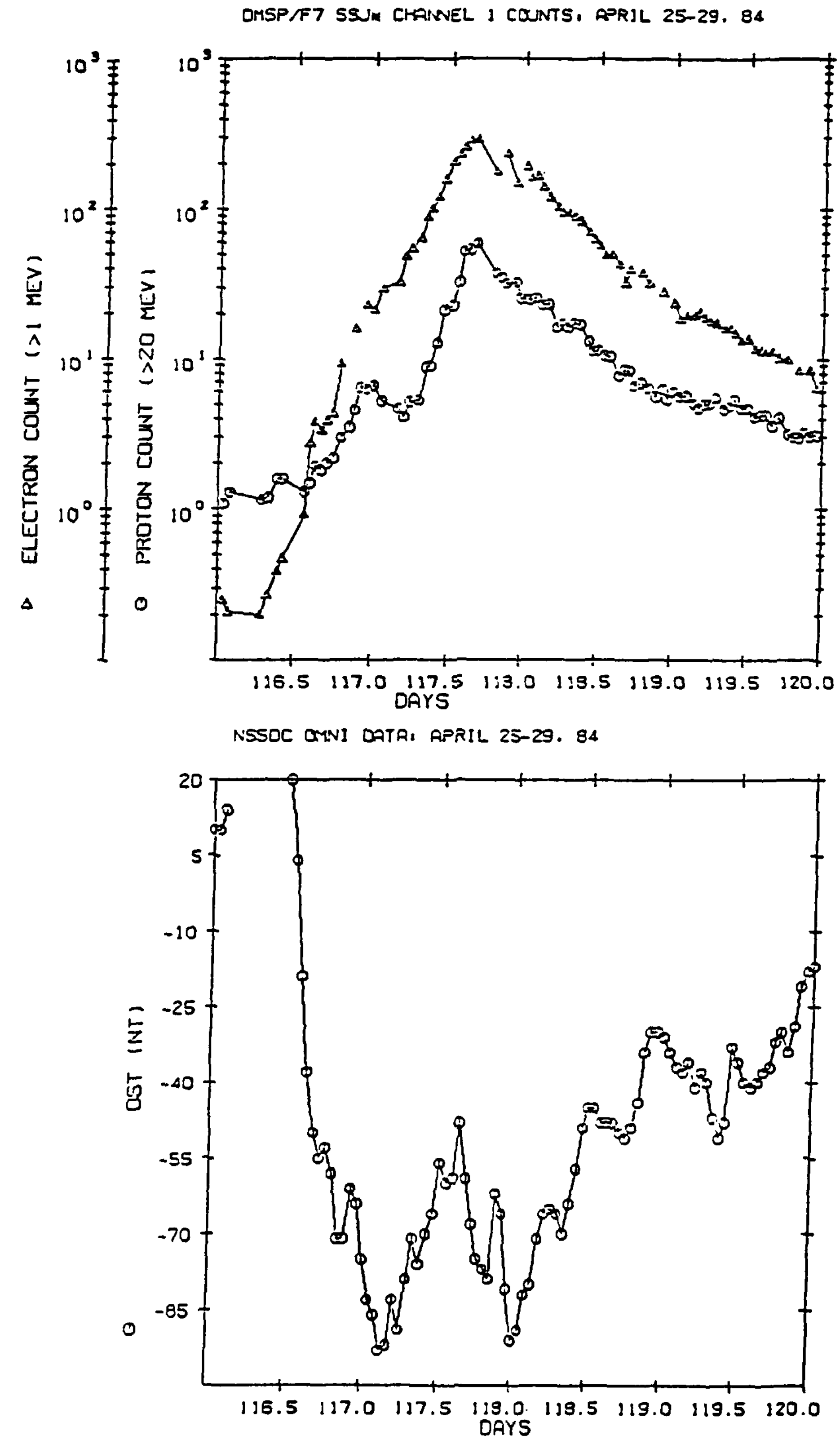

Figure 10. Proton and electron count rates in DMSP/F7 SSJ* instrument during solar particle event of April 24th 1984, and corresponding Dst indices over the time period.

REFERENCES

Armstrong, T. P., "Solar Proton Daily Average Fluxes", University of Kansas, Dept. of Physics and Astronomy preprint, 1989.

Gussenhoven, M. S., Mullen, E. G., Filz, R. C., Hanser, F. A., Lynch, K. A., "Space Radiation Dosimeter SSJ* for the Block 5D/Flight 7 DMSP Satellite: Calibration and Data Presentation", AFGL-TR-86-0065, 20 March 1986, ADA172178.

King, J. H., "Solar Proton Fluences for 1977-1983 Space Missions", J.Spacecraft, 11, No. 6, 401, 1974.

Krimigis, S. M., Armstrong, T. P., Kohl, J. W. D., "Measurements of the Quiet-Time Low Energy Proton, Alpha and M-Nuclei Component in Cosmic Rays", 13th International Cosmic Ray Conference, 2, 1656, 1973.

Mullen, E. G., Gussenhoven, M. S., Lynch, K. A., Brautigam, D., "DMSP Dosimetry Data: A Space Measurement and Mapping of Upset Causing Phenomena", IEEE Trans. on Nuc. Sc., NS-34, No. 6, p. 1251, 1987.

Smith, H. J., and Smith, E. V. P., "Solar Flares", Mc Millan Co., 1963.

Van Allen, J. A., Fennell, J. F., Ness, N. F., "Asymetric Access of Energetic Solar Protons of the Earth's North and South Polar Caps", J. of Geophys. Res., 76, 4262, 1971.

Van Hollebeke, M. A., Ma Sung, L. S., McDonald, F. B., "The Variation of Solar Proton Energy Spectra and Size Distribution with Heliolongitude", Solar Physics, 41, 189, 1975.